Microwave Photonic I/Q Mixer With Phase Shifting Ability

Chan, Erwin; Chen, Hao

Published in:
IEEE Photonics Journal

DOI:
10.1109/JPHOT.2021.3103786

Published: 01/08/2021

Document Version
E-pub ahead of print

Microwave Photonic I/Q Mixer With Phase Shifting Ability

Hao Chen, *Member, IEEE* and Erwin H. W. Chan, *Senior Member, IEEE*

***Abstract*—A compact system with multiple signal processing functions is of interest in many applications. The purpose of this paper is to present a microwave photonic structure that is capable of simultaneously realising in-phase/quadrature (I/Q) mixing and phase shifting operations. The multi-function signal processor has a simple structure and can be constructed using off-the-shelf components. It is designed to enable commercial modulator bias controllers to be incorporated into the system to provide accurate phase shift and to improve system stability. Non-ideal effects in the system that cause deviation in the two output IF signal phase difference from 90° can be mitigated by adjusting a modulator bias voltage. The multi-function signal processor is theoretically analysed and experimentally demonstrated. Its performance including two output IF signals with a quadrature phase difference, wideband operation, continuous 0° to 360° IF signal phase shift and long-term stable operation are verified experimentally.**

***Index Terms*—IQ mixer, optical modulator, phase shifter, bias controller, microwave photonics.**

I. Introduction

There is on-going research in processing microwave and millimetre wave signal in optical domain since 1980s. This is because microwave photonic signal processors have the potential of very wide bandwidth, high reconfigurability, parallel processing and multi-function capabilities [1], [2]. They can also be designed to be compatible with fibre optic communication systems. Microwave frequency mixing is one of the key signal processing functions in many defence and telecommunication systems. Various microwave photonic techniques to realise frequency mixing operation have been reported [3]-[6]. In the past 5 years, research on microwave photonic mixers have been focused on specific mixing functions, e.g. image rejection mixing [7], [8], single sideband mixing [9], [10], subharmonic mixing [11], [12] and in-phase/quadrature (I/Q) mixing [13]-[21], rather than simply demonstrating frequency mixing of two microwave signals or improving microwave photonic mixer performance. Recent research also focuses on including additional functions such as phase shifting operation in a microwave photonic mixer [22], [23].

An I/Q mixer produces two quadrature-phase intermediate frequency (IF) signals by mixing a radio frequency (RF) signal with a local oscillator (LO). It is used in super heterodyne and zero-IF receivers for suppressing interference, microwave phase/frequency discriminators, and Doppler frequency shift (DFS) and phase noise measurement systems [18], [24], [25]. A microwave photonic I/Q mixer can be implemented by a transversal filter approach [13]. It requires controlling the wavelength of two laser sources to alter the optical signal time delay introduced by a dispersive fibre between two Mach Zehnder modulators (MZMs). This I/Q mixer suffers from phase noise, which increases as the RF signal frequency increases. A microwave photonic I/Q mixer can also be implemented by a dual-drive MZM with an asymmetric Mach Zehnder interferometer (AMZI) [14] or a dual-polarisation MZM with a 90° optical hybrid [15], [16]. They have the drawbacks of either require accurate control on the AMZI response to align its notch frequency with the LO sideband frequency and require tuning the AMZI notch frequency as the LO frequency changes, or the output IF signals have considerable phase jitter. Using a wavelength division multiplexer (WDM) to separate the upper and lower sideband of an optical signal from a dual-parallel MZM to realise an I/Q mixing operation is simple [17]. However, commercial modulator bias controllers cannot be used to stabilise the dual-parallel MZM bias points. This is because all commercial bias controllers for dual-parallel MZMs are designed to stabilise the main-MZM in the dual-parallel MZM at the quadrature point, i.e. the main-MZM has a bias angle of 90°, rather than 45° as required in the dual-parallel MZM based I/Q mixer. Bias drift in the dual-parallel MZM alters the quadrature-phase relationship in the two output IF signals. The I/Q mixers based on a dual-polarisation dual-parallel MZM [18] and a dual-polarisation MZM [19] with two sets of polarisation beam splitters (PBSs) and balanced detectors have a complex structure. More importantly, the polarisation state of an optical signal before the PBS needs to be controlled via a polarisation controller to ensure the two output IF signals have a 90° phase difference. The I/Q mixers based on series connection of two optical modulators [20], [21] are only suitable for small signal because the double modulation process generates an unwanted frequency component at the output IF signal frequency. A small input RF signal is needed to ensure this unwanted frequency component has a small amplitude so that it has little effect on the wanted IF signal. Note that the phase of the two output IF signals generated by all the reported I/Q mixers cannot be tuned. Both frequency mixing and phase shifting are required in many systems. It is desirable especially

Manuscript received May 13, 2021; revised July 26, 2021; accepted XX XX, XXXX, Date of publication XX XX, XXXX; date of current version XX XX, XXXX.

Hao Chen and Erwin H. W. Chan are with College of Engineering, IT and Environment, Charles Darwin University, Darwin NT 0909, Australia (e-mail: erwin.chan@cdu.edu.au).

in electronic warfare applications [26] to have a simple structure that can realise these two functions. As such, several microwave photonic topologies for frequency mixing and phase shifting have been reported but none of them can achieve the I/Q mixing operation. Both I/Q mixing and phase shifting operations are needed for beamforming in phased array systems [27], and for a zero-IF transceiver in frequency agile radar, multi-band satellite transponder and wideband wireless communication systems [28].

In this paper, we present a compact microwave photonic structure to realise frequency down conversion with two output IF signals having a quadrature phase difference and phase tuning ability. It is based on a dual-polarisation binary phase shift keying (DP-BPSK) dual-drive MZM and an optical bandpass filter (OBPF) to select the upper sidebands of the modulator output. The two orthogonally polarised upper sidebands are polarisation demultiplexed and routed to two photodetectors, which generate two quadrature-phase IF signals. The IF signal phases can be tuned by adjusting the DP-BPSK modulator bias voltages. Using a commercial DP-BPSK modulator to implement the I/Q mixer enables off-the-shelf bias controllers to be incorporated into the system to provide accurate IF signal phase shift and to improve system stability. Theoretical analysis on the proposed I/Q mixer is presented, which shows that adjusting a modulator bias voltage can suppress the non-ideal effects that affect the I/Q mixer performance. Experimental results are presented that demonstrate the proposed I/Q mixer has a wide operating frequency range of 5 to 18 GHz and a full phase shift range of 0° to 360° with both quadrature phase error and phase shift error of less than ±3°. Using commercial modulator bias controllers in an I/Q mixer and phase shifter structure to obtain a long-term stable performance is also demonstrated for the first time.

II. Operation Principle and Simulation Results

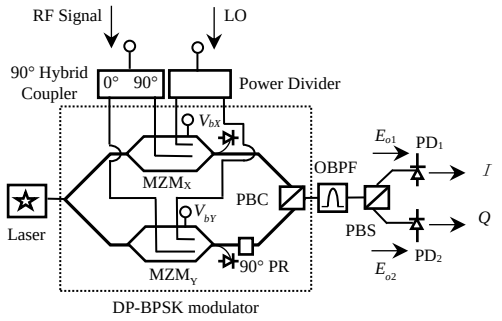

Fig. 1. Schematic diagram of the I/Q mixer with tunable phase.

Fig. 1 shows the structure of the proposed photonics-based I/Q mixer. Continuous wave light from a laser source is launched into a DP-BPSK modulator. The modulator comprises a 3-dB optical coupler, two BPSK modulators (MZM_X and MZM_Y), a 90° polarisation rotator (PR) and a polarisation beam combiner (PBC). It also has two built-in monitor photodiodes (PDs) for automatic bias control for modulator bias drift compensation. An RF signal is fed into a 90° hybrid coupler before injecting into one of the RF ports of MZM_X and MZM_Y. An LO is equally split into two by a power divider and is applied to the other RF ports of MZM_X and MZM_Y. The bias angle of MZM_X and MZM_Y can be controlled by the DC bias voltage V_{bX} and V_{bY} respectively. The output of the DP-BPSK modulator consists of two orthogonal linearly polarised optical signals. The lower sidebands and the optical carrier of the optical signals are filtered out by an OBPF. The upper sidebands of the two orthogonal linearly polarised optical signals are demultiplexed by a PBS. The PBS output electric fields are given by

$$E_{o1}(t)=\frac{1}{2\sqrt{2}}E_{in}\sqrt{t_{ff}}e^{j\omega_c t}\left[\begin{array}{l} J_1(\beta_{RF})e^{j\left(\omega_{RF}t+\frac{\pi}{2}+\phi_1\right)}+J_2(\beta_{RF})e^{j(2\omega_{RF}t+\pi+2\phi_1)} \\ +J_1(\beta_{LO})e^{j(\omega_{LO}t+\phi_2+\beta_X)}+J_2(\beta_{LO})e^{j(2\omega_{LO}t+2\phi_2+\beta_X)}\end{array}\right] \quad (1)$$

$$E_{o2}(t)=\frac{1}{2\sqrt{2}}E_{in}\sqrt{t_{ff}}e^{j\omega_c t}\left[\begin{array}{l} J_1(\beta_{RF})e^{j\omega_{RF}t}+J_2(\beta_{RF})e^{j2\omega_{RF}t} \\ +J_1(\beta_{LO})e^{j(\omega_{LO}t+\beta_Y)}+J_2(\beta_{LO})e^{j(2\omega_{LO}t+\beta_Y)}\end{array}\right] \quad (2)$$

where E_{in} is the electric field amplitude of the continuous wave light into the DP-BPSK modulator, t_{ff} is the insertion loss of each BPSK modulator, $J_n(x)$ is the Bessel function of n^{th} order of the first kind, $\omega_c=2\pi f_c$ is the angular frequency of the optical carrier, $\omega_{LO}=2\pi f_{LO}$ and $\omega_{RF}=2\pi f_{RF}$ are the angular frequency of the LO and RF signal respectively, $\beta_{LO(RF)}=\pi V_{LO(RF)}/V_{\pi,RF}$ is the LO (RF signal) modulation index, $V_{LO(RF)}$ is the voltage of the LO (RF signal) into each electrode of the BPSK modulator, $V_{\pi,RF}$ is the modulator RF port switching voltage, $\beta_{X(Y)}=\pi V_{bX(bY)}/V_{\pi,DC}$ is MZM_X (MZM_Y) bias angle and $V_{\pi,DC}$ is the modulator DC port switching voltage. In practice, 90° hybrid couplers and power dividers have phase imbalance. We include the 90° hybrid coupler phase imbalance ϕ_1 and the power divider phase imbalance ϕ_2 in the analysis to examine how these non-ideal effects affect the I/Q mixer performance. Note that only the first and second order sidebands are considered in the analysis. The higher order sidebands are neglected as they have small amplitudes. (1) and (2) show the amplitude and phase of the positive sidebands from MZM_X and MZM_Y.

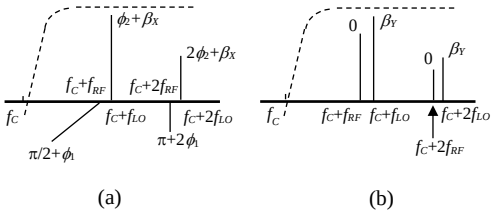

Fig. 2. Spectra of the optical signals into (a) PD_1 and (b) PD_2. Magnitude response of the OBPF (dashed line). f_C: optical carrier frequency, f_{RF}: RF signal frequency, f_{LO}: LO frequency.

The I/Q mixer output optical spectra can be obtained based on (1) and (2) and are shown in Fig. 2(a) and (b). It can be seen from the figure that the phases of the LO sidebands are determined by the bias angles. Both the LO and RF signal sideband phases are affected by the coupler and power divider phase imbalances. The sidebands from MZM_X and MZM_Y are detected by PD_1 and PD_2 respectively. The photocurrent is the product of the PD responsivity $\Re$ and the electric field squared. PD_1 and PD_2 output photocurrent at the IF signal angular

frequency ω_{RF}-ω_{LO} can be obtained from (1) and (2), and are given by

$$I_{o1,IF}(t)=\frac{1}{4}P_{in}t_{ff}\Re J_1(\beta_{RF})J_1(\beta_{LO})\cos\left((\omega_{RF}-\omega_{LO})t+\frac{\pi}{2}+\phi_1-\phi_2-\beta_X\right) \quad (3)$$

$$I_{o2,IF}(t)=\frac{1}{4}P_{in}t_{ff}\Re J_1(\beta_{RF})J_1(\beta_{LO})\cos\left((\omega_{RF}-\omega_{LO})t-\beta_Y\right) \quad (4)$$

where P_{in} is the continuous wave light power into the DP-BPSK modulator. (3) and (4) show the two output IF signals have the same amplitude. The phase of the two output IF signals are $\pi/2+\phi_1-\phi_2-\beta_X$ and $-\beta_Y$. This shows the two IF signal phases can be tuned by controlling MZM_X and MZM_Y bias angles via the modulator bias voltages. Under an ideal situation, i.e. $\phi_1=\phi_2=0°$, an I/Q mixer, i.e. the two output IF signals have a 90° phase difference, can be obtained by ensuring MZM_X and MZM_Y have the same bias angle. A commercial 4-40 GHz bandwidth 90° hybrid coupler and 1-40 GHz bandwidth power divider have a typical phase imbalance of ±5° and ±3° respectively [29]. (3) shows MZM_X bias angle can be adjusted to compensate for the effect of the coupler and power divider phase imbalance. (3) and (4) indicate that the structure shown in Fig. 1 exhibits I/Q mixing with phase shifting ability. A continuous 0° to 360° phase shift in the two output IF signals is realised by changing the bias voltage V_{bX} and V_{bY} from 0 to $2V_{\pi,DC}$. Note that a commercial DP-BPSK modulator has two built-in monitor PDs. This enables the bias angles of MZM_X and MZM_Y to be controlled and stabilised by off-the-shelf modulator bias controllers, e.g. Plugtech MZM bias controller MBC-MZM-01.

Since the two photocurrents at the IF signal frequency have the same amplitude, the electrical power of the two output IF signals are the same and are given by

$$P_{I(Q),out}=\frac{1}{32}P_{in}^2t_{ff}^2\Re^2J_1^2(\beta_{RF})J_1^2(\beta_{LO})R_o \quad (5)$$

where R_o is the PD load resistance. (5) shows the electrical power of the IF signals at the two PD outputs are independent to the modulator bias angles. Hence changing the modulator bias voltages to realise the phase shifting operation has no effect on the IF signal amplitude. The average optical power into the PDs can be obtained from (1) and (2). It is given by

$$P_{ave}=\frac{1}{8}P_{in}t_{ff}\left[J_1^2(\beta_{RF})+J_1^2(\beta_{LO})+J_2^2(\beta_{RF})+J_2^2(\beta_{LO})\right] \quad (6)$$

(6) shows the average output optical power is also independent to the modulator bias angles and is the same for both PBS outputs. (3)-(6) show the second order sidebands do not affect the output IF signal for the I/Q mixer with a sub octave bandwidth and have little effect on the average output optical power under small signal condition. In the case of multi-octave operation, the second order sidebands beat at the PD generates a second order harmonic component, which is located inside the mixer instantaneous bandwidth. This limits the mixer multi-octave spurious free dynamic range performance. Also note that (3)-(6) are also applied for the OBPF designed to pass the lower sidebands while suppress the upper sidebands and the optical carrier.

Note that there are several microwave photonic mixers implemented using a DP-BPSK modulator [30]-[32]. The mixer presented in [30] can realise I/Q mixing but it focuses on improving the conversion efficiency and is unable to realise the phase shifting operation. The mixer presented in [31] can realise phase shifting operation but has a single output. Hence it is not an I/Q mixer. The mixer presented in [32] can realise multichannel phase shifting operation via controlling two orthogonally polarised optical signal polarisation states through a polarisation controller (PC) in front of a polariser. This phase shifting technique requires the polariser to be integrated with the PC in order to obtain a robust performance that is insensitive to environmental perturbations, and the PC needs to be electrically controlled to obtain a specific phase shift. In the proposed structure, the phase shifting operation is realised by controlling the modulator bias voltages. This has the advantages of simplicity, small size and low cost. Furthermore, the proposed structure can be designed to have a long-term stable performance and to eliminate the effect of phase imbalance in the coupler used in the system. These have not been investigated in the reported DP-BPSK modulator based mixers. Note that a high edge roll-off optical filter can select one sideband while largely suppressing the carrier and the unwanted sideband. Using this optical filter in the proposed structure enables the mixer to be operated over a wide frequency range with a lower operating frequency of few GHz. The bandwidth of the proposed I/Q mixer is limited by the 90° hybrid coupler, which is also required in the reported DP-BPSK modulator based mixers [30], [31]. Fortunately, broadband 8-67 GHz 90° hybrid couplers are commercially available. Therefore, the proposed I/Q mixer and phase shifter can operate from the X band to well beyond the Ka band.

III. Experimental Results

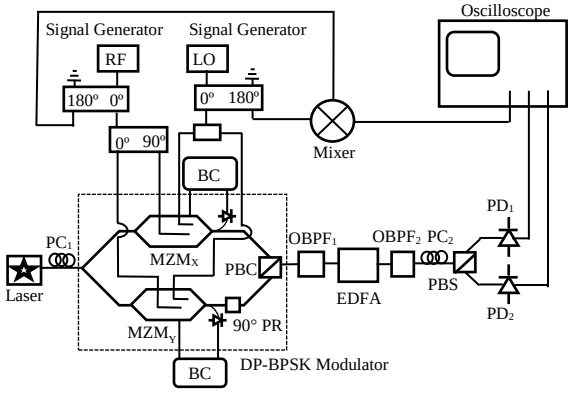

Fig. 3. Experimental setup of the DP-BPSK modulator based I/Q mixer. BC: Bias controller.

The concept of the proposed photonics-based I/Q mixer with phase shifting ability was verified experimentally using the setup shown in Fig. 3. A laser source (Santec WSL-100) generated a 13 dBm 1550 nm continuous wave light. The polarisation state of the continuous wave light was aligned to the slow axis through a polarisation controller (PC_1) before injecting into a DP-BPSK modulator (Fujitsu FTM7980EDA). Two microwave signal generators were used to generate a 11.985 GHz RF signal and a 11.9 GHz LO. The 90° hybrid

coupler (KRYTAR 1830) and the power divider (Gwave GPD-2-020265) used in the experiment had a 3-dB bandwidth of 2-18 GHz and 2-26.5 GHz respectively. Note that two identical 1-18 GHz bandwidth 180° hybrid couplers were connected at the two microwave signal generator outputs. One of the outputs of the two 180° hybrid couplers were connected to an electrical mixer (Minicircuits ZX05-24MH-S+), which generated an IF signal that was used as a reference signal on a 100 MHz four-channel oscilloscope (CRO) (Keysight DSOX2014A). Two modulator bias controllers (Plugtech MBC-MZM-01) were connected to the built-in PDs and the DC bias ports of the DP-BPSK modulator. These bias controllers can stabilise the operating point of an MZM at any point in the modulator transfer function, which not only can enable the realisation of a 0°-360° IF signal phase shift but the desired IF signal phase shift can be maintained over a long period of time. Note that DC power supplies instead of bias controllers can be used to provide DC bias voltages to MZM_X and MXM_Y but the modulator bias drift causes the IF signal phase to change gradually with time.

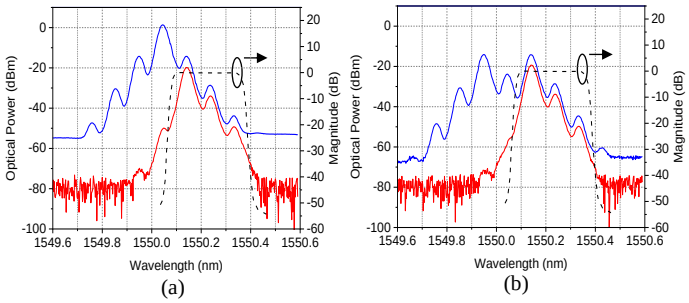

Fig. 4. Normalised magnitude response of $OBPF_1$ (dashed line) and measured optical spectrum before (blue line) and after (red line) $OBPF_1$ when both MZM_X and MZM_Y are operating at (a) the peak bias point and (b) the null bias point.

Fig. 4(a) and (b) show the optical spectrum before and after the tunable optical bandpass filter ($OBPF_1$) when both MZM_X and MZM_Y are biased at the peak point and the null point. $OBPF_1$ magnitude response is also shown by the dashed line in the figures. It can be seen from the figures that $OBPF_1$ largely suppresses the optical carrier and the lower sidebands. Note that the horizontal axis in Fig. 4 is in wavelength. Therefore, the upper sidebands in frequency were suppressed, and the first order lower sideband in frequency was the dominant optical component, which determines the average output optical power. Its amplitude remains the same for different MZM_X and MZM_Y bias angles. $OBPF_1$ was followed by an erbium-doped fibre amplifier (EDFA) and a 0.5 nm 3-dB bandwidth optical bandpass filter ($OBPF_2$) to compensate for the system loss and to suppress the amplified spontaneous emission (ASE) noise. A polarisation controller (PC_2) after $OBPF_2$ was adjusted to align the polarisation states of the two orthogonally polarised optical signals to the slow and fast axis before launching to a PBS. This ensures one of the PBS outputs consists of the optical signal from MZM_X only while the other PBS output consists of the optical signal only from MZM_Y. Two PDs (Discovery Semiconductors DSC30S) with bandwidths of 20 GHz and responsivities of 0.8 A/W were connected to the PBS outputs. The IF signals generated by the two PDs were measured in both frequency and time domain on an electrical signal analyser (ESA) (Keysight N9000A) and an CRO.

The transfer functions of MZM_X and MZM_Y inside the DP-BPSK modulator were measured in advance. This was done by measuring the DP-BPSK modulator average output optical power while sweeping MZM_X bias voltage from -10 V to 10 V while MZM_Y was biased at the null point and vice versa. The results show MZM_X and MZM_Y have a switching voltage of 8.7 V and 8.54 V respectively. The peak bias voltage of MZM_X and MZM_Y are -0.1 V and -1 V respectively. The difference of these two voltages was used as a bias offset for the phase shift measurement.

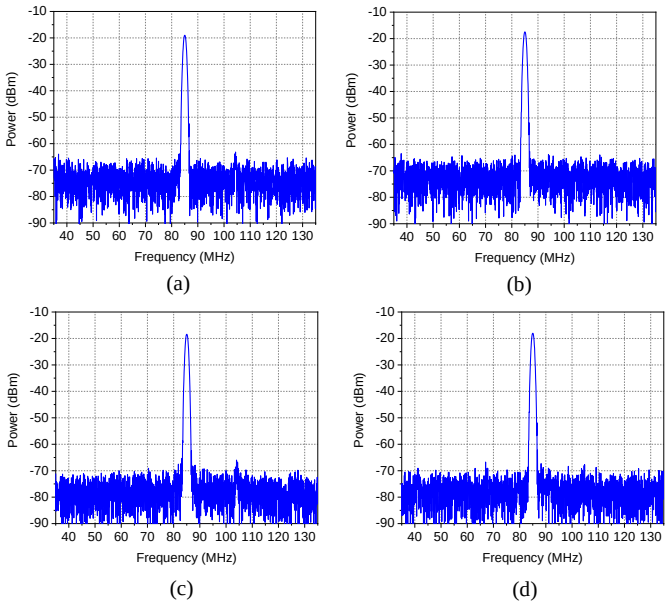

Fig. 5. Measured electrical spectra at the I/Q mixer (a) PD_1 and (b) PD_2 output when both MZM_X and MZM_Y are biased at the peak point. Measured electrical spectra at the I/Q mixer (c) PD_1 and (d) PD_2 output when both MZM_X and MZM_Y are biased at the null point.

Fig. 5(a) and (b) show the electrical spectra of the two I/Q mixer outputs when both MZM_X and MZM_Y were biased at the peak point. The power of the two output IF signals at 85 MHz are around -19.5 dBm. The middle and bottom trace of Fig. 6(a) show the two IF signal waveforms measured on the CRO. The phase difference of the two IF signals can be obtained using the phase measurement function on the CRO and is found to be 91°. The above measurements were repeated after biasing both MZM_X and MZM_Y at the null point. Fig. 5(c) and (d) show the IF signal powers remain almost the same, i.e. -19.5 dBm, after changing the modulator bias voltages. More importantly, the middle and bottom trace of Fig. 6(b) show the phase difference of the two IF signals remains 91° and the two IF signals have a 180° phase shift compared to that in Fig. 6(a). This demonstrates the realisation of I/Q mixing with phase shifting operation.

The phase shifting operation of the proposed I/Q mixer was investigated. Initially, both MZM_X and MZM_Y were biased at the peak point (V_{bX}=-0.1 V and V_{bY}=-1 V). Under this condition, PD_1 and PD_2 output electrical spectra are shown in Fig. 5(a) and

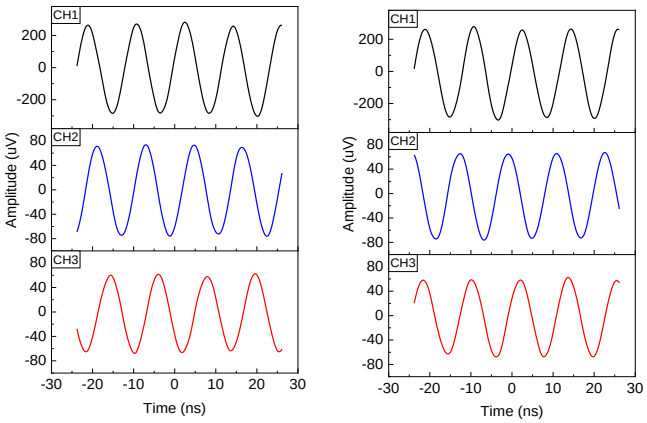

Fig. 6. IF signal waveforms measured at PD_1 (middle trace) and PD_2 (bottom trace) output when both MZM_X and MZM_Y are biased at (a) the peak point and (b) the null point. A reference IF signal waveform measured at the electrical mixer output is shown in the top trace.

(b) and the IF signal waveforms, which have a 91° phase difference, are shown in Fig. 6(a). The phase shift of the IF signals from PD_1 and PD_2 relative to the reference IF signal from the electrical mixer were measured on the CRO and are normalised to be 0° and 91° respectively as shown by the arrows in Fig. 7(a). The IF signal phase shifts were measured for different MZM_X and MZM_Y bias voltages. Fig. 7(a) shows PD_2 output IF signal phase increases linearly from -180° to +180° when MZM_Y bias voltage changes from -9.56 V to 7.56 V. At the same time, changing MZM_X bias voltage from -8.8 V to 8.6 V causes -88° to 269° PD_1 output IF signal phase change. This demonstrates the phase of the IF signals can be controlled by the modulator bias voltages. Furthermore, the two IF signal phase difference can be maintained at 90° with less than 3° errors as shown in Fig. 7(b). This verifies the proposed structure has both I/Q mixing and phase shifting functions. Note that the difference of the two modulator bias voltages is around 1 V to ensure the IF signals have a quadrature phase relationship. This agrees with the bias offset value obtained from MZM_X and MZM_Y transfer function measurement. This verifies that a 90° IF signal phase difference is obtained by setting the two BPSK modulators to have almost the same bias angle. Fig. 8 shows the two output IF signal peak-to-peak voltages measured on the CRO have less than 8 μV change when adjusting the modulator bias voltages to tune the IF signal phases. This demonstrates that the phase shifting operation has very little effect on the output IF signal amplitudes. Note that, due to the bandwidth limitation of the CRO used in the experiment, the I/Q mixer phase shifting ability can only be demonstrated at an IF signal frequency of less than 100 MHz. There is no problem for the proposed structure to operate at a higher IF signal frequency of few hundred megahertz or even a gigahertz for electronic warfare applications [33], as long as the PD bandwidth is wide enough to cover the IF signal frequency. Since a bias controller is required in all photonics-based frequency mixers that involve optical modulators for stabilising the modulator bias point, controlling the modulator bias voltage via a bias controller to implement the phase shifting operation does not increase the system size and cost. This also avoids the frequency-dependent phase shift problem when using an electronic phase shifter after the PD to realise the phase shifting operation.

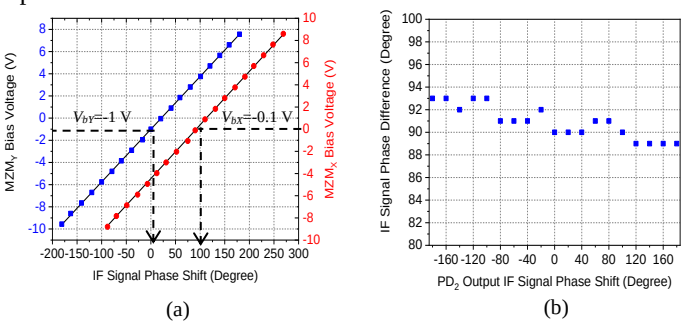

Fig. 7. (a) Predicted (solid line) and measured MZM_X (red dots) and MZM_Y (blue squares) bias voltage versus the phase of PD_1 and PD_2 output IF signal relative to the reference IF signal phase. (b) PD_1 and PD_2 output IF signal phase difference for different PD_2 output IF signal phases obtained by adjusting MZM_X and MZM_Y bias voltages shown in (a).

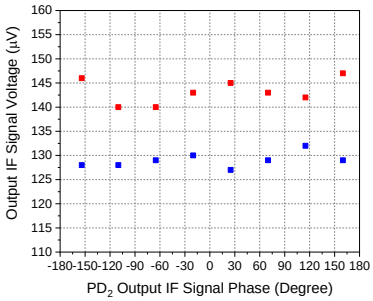

Fig. 8. PD_1 (red square) and PD_2 (blue square) output IF signal peak-to-peak voltages for different PD_2 output IF signal phases.

The RF signal frequency was changed from 11.905 GHz to 11.995 GHz while the LO frequency was fixed at 11.9 GHz to examine the proposed I/Q mixer performance for different output IF signal frequencies. Both MZM_X and MZM_Y were biased at the peak point. Fig. 9 shows the proposed I/Q mixer conversion efficiency, which is the ratio of the output IF signal power to the input RF signal power, and the phase difference of the two output IF signals, versus the IF signal frequency. The figures show the two I/Q mixer outputs have a conversion efficiency of around -16 dB and -16.8 dB. There is less than 1 dB change in the conversion efficiency and only 1° phase difference variation in the two output IF signals as the IF signal frequency changes from 5 to 95 MHz.

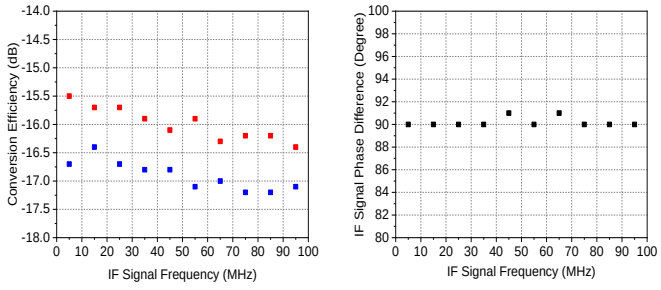

Fig. 9. (a) Measured I/Q mixer conversion efficiency at PD_1 output (red square) and PD_2 output (blue square) for different IF signal frequencies. (b) Measured IF signal phase difference for different IF signal frequencies.

In order to demonstrate the proposed I/Q mixer is capable to operate over a wide frequency range, the conversion efficiency and the IF signal phase difference were measured for different input RF signal frequencies. The LO frequency was changed accordingly to fix the IF signal frequency at 85 MHz. The measurement in Fig. 10(a) shows the conversion efficiency of the I/Q mixer at the two PD outputs has less 1.5 dB change over a 13 GHz frequency range from 5 GHz to 18 GHz. There is around 1 dB difference in conversion efficiency of the two PD outputs, which can be eliminated by adjusting the optical power into the PDs. Fig. 10(b) shows the IF signal phase difference remains 90° with ±1° error for different input RF signal frequencies.

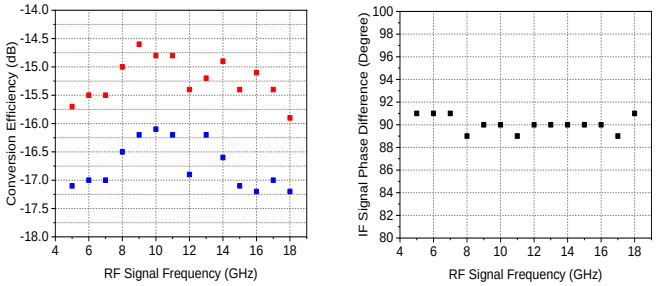

(a) (b)

Fig. 10. (a) Measured I/Q mixer conversion efficiency at PD_1 output (red square) and PD_2 output (blue square) for different RF signal frequencies. (b) Measured IF signal phase difference for different RF signal frequencies.

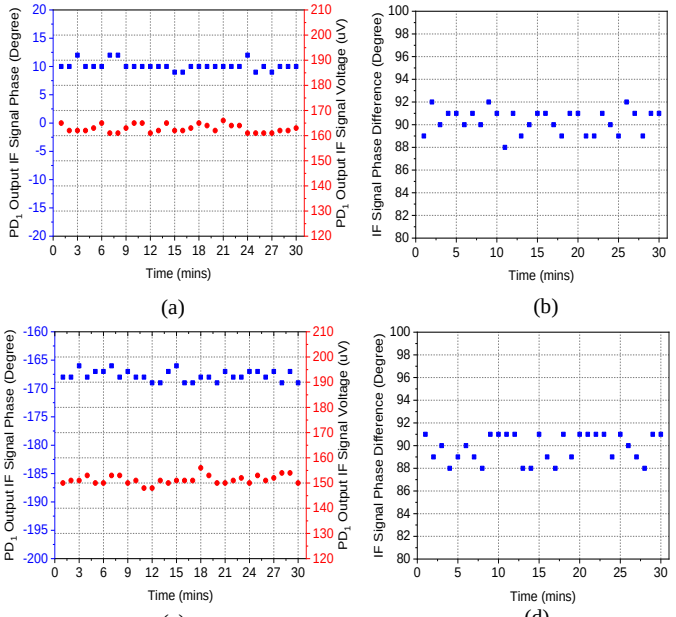

(a) (b)

(c) (d)

Fig. 11. Stability measurement of PD_1 output IF signal phase relative to the reference IF signal phase (blue square) and PD_1 output IF signal peak-to-peak voltage (red square), and stability measurement of the two output IF signal phase difference, when both MZM_X and MZM_Y are biased at the peak point ((a), (b)) and the null point ((c), (d)).

An important advantage of the proposed I/Q mixer is that off-the-shelf modulator bias controllers can be used to lock the operating point of the DP-BPSK modulator to obtain a long-term stable performance. To verify this, the RF signal and LO frequencies were set at 11.985 GHz and 11.9 GHz respectively. Both MZM_X and MZM_Y were biased at the peak point. PD_1 output IF signal waveform peak-to-peak voltage and phase relative to the reference IF signal phase were measured on the CRO every minute for 30 minutes. The measurements are shown in Fig. 11(a). Fig. 11(b) shows the two PD output IF signal phase difference stability measurement. The measurements shown in Fig. 11(a) and (b) were repeated after adjusting MZM_X and MZM_Y bias voltages via the bias controllers so that both MZM_X and MZM_Y were biased at the null point. The corresponding results are shown in Fig. 11(c) and (d). Fig. 11 shows the output IF signal peak-to-peak voltage has less than 10 μV change over 30 minutes. The output IF signal phase can be maintained within ±2° relative to the reference IF signal phase. Fig. 11(a) and (c) show PD_1 output IF signal phase is changed from 10°±2° to -168°±2° when changing the two BPSK modulator bias angles from 0 to π. This 180° phase change agrees with theory. Fig. 11(b) and (d) show the phase difference of the two output IF signals is maintained at 90°±2° over 30 minutes.

IV. Conclusion

A microwave photonic structure based on a DP-BPSK modulator and an OBPF, that is capable to realise frequency down conversion with two phase-tunable quadrature-phase IF signals, has been presented. Adjusting the modulator bias voltages not only can shift the two output IF signal phases without altering their amplitudes, but it can also mitigate the effect of the coupler and power divider phase imbalance on the output IF signals. The I/Q mixer and phase shifter structure is designed to enable commercial bias controllers to be incorporated into the system to eliminate the modulator bias drift problem. It should be emphasised that the bias drift problem in many microwave photonic signal processors based on a dual-parallel MZM structure cannot be solved by using commercial bias controllers. This is because commercial bias controllers for dual-parallel MZMs can only lock the sub-MZMs and the main-MZM at the null and quadrature point respectively. Experimental results have been presented that demonstrate, for the first time, a microwave photonic structure exhibits wideband and long-term stable I/Q mixing and phase shifting operation. The phase shift errors and the errors in the two output IF signal phase difference are less than ±3°. The measured IF signal phase shifts for different modulator bias voltages are in excellent agreement with predictions.

References

[1] R. A. Minasian, E. H. W. Chan, and X. Yi, "Microwave photonic signal processing," *Opt. Exp.*, vol. 21, no. 19, pp. 22918–22936, 2013.

[2] R. A. Minasian, "Ultra-wideband and adaptive photonic signal processing of microwave signals," *IEEE J. Quant. Elect.*, vol. 52, no. 1, pp. 0600816, 2016.

[3] G. K. Gopalakrishnan, R. P. Moeller, M. M. Howerton, W. K. Burns, K. J. Williams, and R. D. Esman, "A low-loss downconverting analog fiber-optic link," *IEEE Trans. Microwave Theory Tech.*, vol. 43, no. 9, pp. 2318-2323, 1995.

[4] Y. Li, R. Wang, J. S. Klamkin, L. A. Johansson, P. R. Herczfeld and J. E. Bowers, "Quadratic electrooptic effect for frequency down-conversion," *IEEE Trans. Microwave Theory Tech.*, vol. 58, no. 3, pp. 665-673, 2010.

[5] B. M. Haas and T. E. Murphy, "Linearized downconverting microwave photonic link using dual-wavelength phase modulation and optical filtering," *IEEE Photon. J.*, vol. 3, no. 1, pp. 1-12, 2011.
[6] E. H. W. Chan and R. A. Minasian, "Microwave photonic downconverter with high conversion efficiency," *J. Lightwave Technol.*, vol. 30, no. 23, pp. 3580-3585, 2012.
[7] P. Li, W. Pan, X. Zou, B. Lu, L. Yan and B. Luo, "Image-free microwave photonic down-conversion approach for fiber-optic antenna remoting," *IEEE Journal of Quantum Electronics*, vol. 53, no. 4, 9100208, 2017.
[8] C. B. Albert, C. Huang, and E. H. W. Chan, "Brillouin-assisted notch filtering based all-optical image rejection mixer," *IEEE Photon. J.*, vol. 11, no. 2, 7202712, 2019.
[9] Y. Wang, J. Xu, D. Wang, T. Zhou, D. Yang, X. Zhong, and F. Yang, "Microwave photonic mixer with large mixing spurs suppression and high RF/LO isolation," *Optik.*, vol. 174, pp. 630–635, 2018.
[10] C. Huang, E. H. W. Chan, and C. B. Albert, "A compact photonics-based single sideband mixer without using high-frequency electrical components," *IEEE Photon. J.*, vol. 11, no. 4, 7204509, 2019.
[11] E. Rouvalis, M. J. Fice, C. C. Renaud, and A. J. Seeds, "InP-based ultra-fast photodetectors for millimeter-wave sub-harmonic mixers," P*roc. Int. Top. Meet. Microw. Photon.*, pp. 57–59, 2011.
[12] J. Zhang, E. H. W. Chan, X. Wang, X. Feng, and B. Guan, "Broadband microwave photonic sub harmonic downconverter with phase shifting ability," *IEEE Photon. J.*, vol. 9, no. 3, 5501910, 2017.
[13] H. Emami and N. Sarkhosh, "Reconfigurable microwave photonic in-phase and quadrature detector for frequency agile radar," *J. Opt. Soc. Am.*, A vol. 31, pp. 1320-1325, 2014.
[14] S. T. Lipkowitz, T. U. Horton, and T. E. Murphy, "Wideband microwave electro-optic image rejection mixer," *Opt. Lett.*, vol. 44, no. 19, pp. 4710-4713, 2019.
[15] Z. Tang and S. Pan, "Reconfigurable microwave photonic mixer with minimized path separation and large suppression of mixing spurs," *Opt. Lett.*, vol. 42, no. 1, pp. 33-36, 2017.
[16] Z. Tang and S. Pan, "A Reconfigurable photonic microwave mixer using a 90° optical hybrid," *IEEE Trans. Microwave Theory Tech.*, vol. 64, no. 9, pp. 3017-3025, 2016.
[17] Y. Gao, A. Wen, W. Chen, and X. Li, "All-optical, ultra-wideband microwave I/Q mixer and image-reject frequency down-converter," *Opt. Lett.*, vol. 42, no. 6, pp. 1105-1108, 2017.
[18] Y. Gao, A. Wen, W. Jiang, Y. Fan, and Y. He, "All-optical and broadband microwave fundamental/sub-harmonic I/Q down-converters," *Opt. Express*, vol. 26, no. 6, pp. 7336-7350, 2018.
[19] Y. Gao, A. Wen, W. Zhang, W. Jiang, J. Ge, and Y. Fan, "Ultra-wideband photonic microwave I/Q mixer for zero-IF receiver," *IEEE Trans. Microwave Theory Tech.*, vol. 65, no. 11, pp. 4513-4525, 2017.
[20] M. Lei, Z. Zheng, J. Qian, X. Gao, and S. Huang, "All-optical microwave I/Q mixer based on cascaded phase modulator and dual-drive Mach–Zehnder modulator," *Optical Fiber Communication Conference (OFC) 2019*, paper Th3C.3, 2019.
[21] J. Shi, F. Zhang, D. Ben, and S. Pan, "Wideband microwave photonic I/Q mixer based on parallel installed phase modulator and Mach-Zehnder modulator," *2018 IEEE MTT-S International Wireless Symposium (IWS)*, pp. 1-4, 2018.
[22] T. Jiang, S. Yu, R. Wu, D. Wang, and W. Gu, "Photonic downconversion with tunable wideband phase shift," *Opt. Lett.*, vol. 41, no. 11, pp. 2640-2643, 2016.
[23] T. Li, E. H. W. Chan, X. Wang, X. Feng, B. Guan, and J. Yao, "Broadband photonic microwave signal processor with frequency up/down conversion and phase shifting capability," *IEEE Photon. J.*, vol. 10, no. 1, 5500112, 2018.
[24] S. Pan and J. Yao, "Photonics-based broadband microwave measurement," *J. Lightwave Technol.*, vol. 35, no. 16, pp. 3498-3513, 2017.
[25] J. Shi, F. Zhang, D. Ben, and S. Pan, "Wideband microwave phase noise analyzer based on an all-optical microwave I/Q mixer," *J. Lightwave Technol.*, vol. 36, no. 19, pp. 4319-4325, 2018.
[26] J. Y. Choe, "Defense RF systems: future needs, requirements, and opportunities for photonics," *Proc. Int. Top. Meet. Microw. Photon.*, pp. 307-310, 2005.
[27] Y. Yu, P. G. M. Baltus, A. de Graauw, E. van der Heijden, C. S. Vaucher, and A. H. M. van Roermund, "A 60 GHz phase shifter integrated with LNA and PA in 65 nm CMOS for phased array systems," *IEEE Journal of Solid-State Circuits*, vol. 45, no. 9, pp. 1697-1709, 2010.
[28] Y. Gao and W. Jiang, "Wideband photonic RF transceiver with zero-IF architecture," *2017 International Topical Meeting on Microwave Photonics (MWP)*, pp. 1-4, 2017.
[29] Marki Microwave 3 dB quadrature hybrid (QH-0440) and ultra-wideband Wilkinson power divider (PD-0140) datasheets, (2019), www.markimicrowave.com
[30] J. Zhang, E. H. W. Chan, X. Wang, X. Feng, and B. Guan, "High conversion efficiency photonic microwave mixer with image rejection capability," *IEEE Photon. J.*, vol. 8, no. 4, 3900411, 2016.
[31] T. Jiang, R. Wu, S. Yu, D. Wang, and W. Gu, "Microwave photonic phase-tunable mixer," *Opt. Express*, vol. 25, no. 4, pp. 4519-4527, 2017.
[32] Y. Gao, A. Wen, Z. Tu, W. Zhang, and L. Lin, "Simultaneously photonic frequency downconversion, multichannel phase shifting, and IQ demodulation for wideband microwave signals," *Opt. Lett.*, vol. 41, no. 19, pp. 4484-4487, 2016.
[33] M. E. Manka, "Microwave photonics for electronic warfare applications," *IEEE International Topical Meeting on Microwave Photonics (MWP 2008)*, pp. 275-278, 2008.